International Journal of Thermophysics, Vol. 28, No. 4, August 2007 (© 2007)
DOI: 10.1007/s10765-007-0203-1

Modeling of the Effective Thermal Conductivity of Consolidated Porous Media with Different Saturants: A Test Case of Gabbro Rocks

Aurangzeb[1] **and A. Maqsood**[1,2]

Received December 2, 2006

The thermal conductivity and thermal diffusivity of porous consolidated gabbro rocks have been measured simultaneously by the transient plane source technique at normal temperature and pressure using air and water as saturants. The density and porosity are measured using American Society for Testing and Materials (ASTM) standards under ambient conditions. The mineral composition is obtained using a petrography technique. Data are presented for 12 specimens of gabbro, taken from Warsik near Peshawar, Pakistan. A recently proposed empirical model for the prediction of the thermal conductivity of porous consolidated igneous rocks is established using different fluids in pore spaces, under ambient conditions. An exponential decay formula is also proposed for the prediction of the thermal conductivity at room temperature and normal pressure. The results are compared with different existing empirical models. A simple correlation between density and porosity is also reported.

KEY WORDS: density; gabbro; mixing law models; porosity; thermal conductivity; transient plane source technique.

1. INTRODUCTION

A knowledge of the thermal transport properties of rocks has become important with the widespread interest in thermal processes, e.g., underground fluid-bearing reservoirs. Some of these processes include thermal methods of enhanced oil recovery, management of geothermal reservoirs,

[1] Thermal Physics Laboratory, Department of Physics, Quaid-i-Azam University, Islamabad 45320, Pakistan.
[2] To whom correspondence should be addressed. E-mail: tpl.qau@usa.net

and underground disposal of nuclear waste. The design of thermal-insulating materials also depends upon the heat transfer characteristics of porous media.

Precise measurements of the thermal conductivity of rocks are difficult to make and are very time-consuming. To make laboratory measurements on all types of rocks of interest and under all environmental conditions of temperature, pressure, and fluid saturation would be prohibitive in terms of time and expense. Consequently, a lot of effort [1–20] has been made to devise a simple physical model for the prediction of thermal conductivities of porous rocks filled with fluids ranging in thermal conductivity from that of air to that of water.

Igneous rocks are classified on the basis of texture and chemistry. On the basis of texture (grain size), igneous rocks are divided into two groups [21]: extrusive, volcanic, or fine grained and intrusive, plutonic, or coarse grained. On the basis of chemical composition, igneous rocks fall into four groups: felsic, intermediate, mafic, and ultramafic. Gabbro lies in the coarse-grained mafic category of igneous rocks. In these rocks, silica amounts from 45 to 52% (by volume).

The present work presents thermal parameters of 12 porous specimens of gabbro, ranging in porosity from 0.322 to 0.935% by volume, taken from Warsik near Peshawar, located in the north of Pakistan. The porosity and density parameters are measured using American Society for Testing and Materials (ASTM) standards, under ambient conditions. The mineralogical composition is found by making thin sections of specimens (petrography), while the thermal transport properties are measured using the transient plane source (TPS) technique [22] at normal temperature and pressure. The thermal conductivity of a given piece of rock depends, at constant temperature and pressure, on the mineralogical composition, as well as on its porosity and pore filling (which can be air, water, oil, etc.) and also on the geometrical composition. The aim of the present work is to model the thermal conductivity of porous consolidated igneous rocks in terms of easily measurable parameters such as porosity, thermal conductivity of fluid contained in pores, and thermal conductivity of their constituent solid phase.

2. ESTIMATION OF THERMAL CONDUCTIVITY

Three basic types of models for the estimation of the thermal conductivity of multi-component systems have been used in the past [23]. The first type involves the application of mixing laws for porous mineral aggregates containing various fluids. Since, these models do not take into account the structural characteristics of rocks, they are of limited

applicability. A second type is the empirical model in which more easily measured physical properties are related to thermal conductivity through the application of regression analysis to laboratory data. This method also has its shortcomings in the sense that the resulting model may be applicable only to the particular suite of rocks being investigated. The third type is the theoretical model based on the mechanisms of heat transfer applicable to simplified geometries of the rock/fluid system. The difficulty here is the degree of simplification necessary to obtain a solution.

The proposed models have limited applicability and cannot be used for all types of systems, especially when the differences in the thermal conductivities of the constituent phases are very large. A general expression to predict the effective thermal conductivity is still lacking.

If we assume that the constituent minerals with thermal conductivities λ_i and volume concentrations V_i are arranged in parallel in a non-porous rock, then the thermal conductivity λ_s of the pure solid phase will be

$$\lambda_s = \frac{\Sigma \lambda_i V_i}{\Sigma V_i} \tag{1}$$

In the following section, we will discuss some of the mixing laws and empirical models.

2.1. Mixing Law Models

Three very basic mixing-law models [23] are given as follows.

2.1.1. Weighted Arithmetic

This mixing law suggests the parallel arrangement of components (solid and fluid phases) relative to the direction of heat flow and gives the maximum value of the effective thermal conductivity, and is expressed as

$$\lambda_e = \Phi \lambda_f + (1 - \Phi) \lambda_s, \tag{2}$$

where Φ is the fractional porosity and λ_f is the thermal conductivity of the fluid contained in pore spaces.

2.1.2. Weighted Harmonic

This mixing law suggests the perpendicular arrangement of components relative to the direction of heat flow and gives the minimum value of the effective thermal conductivity, and is expressed as

$$\lambda_e = \left(\frac{\Phi}{\lambda_f} + \frac{1 - \Phi}{\lambda_s} \right)^{-1} \tag{3}$$

2.1.3. Weighted Geometric

This mixing law [24] has no physical background but gives better results compared with Eqs. (1) and (2). It is expressed as

$$\lambda_e = \lambda_s \left(\frac{\lambda_f}{\lambda_s} \right)^{\Phi}, \tag{4}$$

where all the variables are defined as above.

2.2. Empirical Models

In developing the empirical models, more easily measured physical parameters are related to thermal conductivity with the addition of some empirical coefficients, exponents, or adjustable parameters, whose values can be determined from a least-squares fit to laboratory data. Some examples are given below.

2.2.1. Asaad's Model

Asaad's equation [2] is very similar to the weighted geometric mean model, given as

$$\lambda_e = \lambda_s \left(\frac{\lambda_f}{\lambda_s} \right)^{c\Phi}, \tag{5}$$

where c is an empirical exponent. When $c = 1$, this equation becomes identical to Eq. (4).

2.2.2. Sugawara and Yoshizawa Model

The Sugawara and Yoshizawa [6] model is expressed as

$$\lambda_e = (1 - A)\lambda_s + A\lambda_f, \tag{6}$$

where $A = \left(\left\{ \frac{2^n}{2^n - 1} \right\} \left\{ 1 - \frac{1}{(1+\Phi)^n} \right\} \right)$ is an adjustable parameter and $n(>0)$ is the empirical exponent depending on the porosity, shape, orientation, and emissivity inside the pores.

2.2.3. Veerendra and Chaudhary Model

For porous consolidated materials, the extended Veerendra and Chaudhary model [12] is

$$\lambda_e = (1 - \Phi)\,\lambda_H + \Phi\lambda_L - \psi \left(\frac{\lambda_s}{\lambda_f} \right)^{\frac{1}{3}} \tag{7}$$

where $\lambda_H = \lambda_s e^{\beta\Phi}$ and $\lambda_L = \lambda_f e^{-\beta(1-\Phi)}$ for $\lambda_s > \lambda_f$ and $\beta = \left(\frac{\lambda_f}{\lambda_s} - 1\right)$.

According to Veerendra and Chaudhary, there is a corrective term, $\Phi(1-\Phi)\sqrt{\lambda_L \lambda_H}$, which may be either added or subtracted from Eq. (7). The term $\psi\left(\frac{\lambda_s}{\lambda_f}\right)^{\frac{1}{3}}$ is to account for a high thermal conductivity ratio $\left(\frac{\lambda_s}{\lambda_f}\right)$. The coefficient ψ is determined to conform to the experimental results.

2.2.4. Pande and Chaudhary Model

For porous consolidated materials, the model proposed by Pande and Chaudhary [14] is

$$\lambda_e = F\,(0.6132)\,(\lambda_s \lambda_f)^{\frac{1}{2}} \left(1 - 1.545\xi_f^{\frac{2}{3}}\right) \quad \text{for} \quad \xi_f > 0 \tag{8}$$

$$\lambda_e = F\,(0.6132)\,(\lambda_s \lambda_f)^{\frac{1}{2}} \left(1 + 3.844\xi_s^{\frac{2}{3}}\right) \quad \text{for} \quad \xi_s > 0 \tag{9}$$

where $\xi_f = \Phi - 0.5$, $\xi_s = 0.5 - \Phi$, and F is an empirical coefficient determined to conform with the material studied.

A recently proposed empirical model [25] for the prediction of thermal conductivity of consolidated porous media in terms of easily measurable parameters is

$$\frac{1}{\lambda_e} = \frac{1}{\lambda_s} + \frac{m\Phi}{\lambda_f}, \tag{10}$$

where m is the empirical coefficient whose value can be determined using experimental values of thermal conductivity and the corresponding values of Φ and λ_s, by

$$m = \lambda_f \left(\frac{\sum\left(1/\lambda_{exp} - 1/\lambda_s\right)}{\sum \Phi}\right) \tag{11}$$

The empirical coefficients, exponents, or adjustable parameters may vary according to the suite of rocks. Therefore, the extrapolations of empirical models to suites of rocks other than those used in developing these models may not be satisfactory.

3. MEASURING TECHNIQUES AND SAMPLE CHARACTERIZATION

The samples were collected with the collaboration of the Geological Survey of Pakistan (GSP), Islamabad and were cut in rectangular shapes

having approximate dimensions of $4.5 \times 4.5 \times 2.5\,\text{cm}^3$. There were 12 specimens with four samples of each type. The average values of the measurements are stated here.

For density-related parameters, the specimens were dried at $(105 \pm 5)^\circ\text{C}$ in a furnace for 24 h. After drying, the specimens were cooled at room temperature for 30 min and then kept in desiccators. For mass measurements, a digital balance with a tolerance of 0.001 g was used. The volume of each sample was determined within $0.001\,\text{cm}^3$.

The transient plane source (TPS) technique, also known as Gustafsson's probe [22] was used to measure the thermal conductivity of these materials because it allows measurements without any disturbance from the interfaces between the sensor and the bulk specimens. Also, simultaneous measurements of the thermal conductivity, thermal diffusivity, and heat capacity per unit volume are possible [26]. In this technique, a TPS-element is used both as a constant heat source and a sensor of temperature. For data collection the TPS-element (20 mm diameter) sandwiched between two specimen halves in a bridge circuit [27,28] was used. When a sufficiently large amount of direct current is passed through the TPS-element, its temperature changes consequently and there is a voltage drop across the TPS-element. By recording this voltage drop for a particular time interval, detailed information about the thermal conductivity (λ) and thermal diffusivity (κ) of the test specimen is obtained. The heat capacity per unit volume (ρC_p) is then calculated from the relation,

$$\rho C_P = \frac{\lambda}{\kappa}, \tag{12}$$

where ρ is the density of the samples.

Taking into consideration the errors of the technique [28,29], standard deviations of the measurements, and the sampling errors, the uncertainties in the thermal conductivity and thermal diffusivity data are estimated to be 5 and 7%, respectively. The uncertainty in the volumetric heat capacity is approximately 10%.

4. RESULTS AND DISCUSSION

Thermal properties of porous rocks depend upon their structure, mineral composition, porosity, density, the ability of their constituent minerals to conduct heat, etc. Grain density (ρ_s), bulk density (ρ), and porosity are grouped as the density-related properties of rocks. The results of the experiments are discussed in the following.

Table I. Measured Fractional Porosity (Φ), Bulk Density (ρ_o), and Estimated Density (ρ_{est}) of Gabbro Specimens at Normal Temperature and Pressure

S. No.	Φ	ρ_0 $(10^3\,\text{kg}\cdot\text{m}^{-3})\pm 0.002$	ρ_{est} $(10^3\,\text{kg}\cdot\text{m}^{-3})$
Gb01	0.00322	2.974	2.905
Gb02	0.00332	2.922	2.904
Gb03	0.00413	2.975	2.902
Gb04	0.00468	2.986	2.900
Gb05	0.00637	3.031	2.895
Gb06	0.00655	3.020	2.895
Gb07	0.00783	2.992	2.891
Gb08	0.00850	2.943	2.889
Gb09	0.00855	2.961	2.889
Gb10	0.00894	2.995	2.888
Gb11	0.00905	2.914	2.888
Gb12	0.00935	3.178	2.887

4.1. Density-Related Properties

The density of rocks depends on their mineral composition and structure. From thin sections of the specimens, it is found that on the average, these samples consist of 69% calcium-rich plagioclase feldspars, 20% pyroxene, 6% olivine, and 5% amphibole by volume. Their densities are 2.769, 3.209, 3.469, and $3.059\,\text{g}\cdot\text{cm}^{-3}$, respectively [30]. Thus, the density of the solid phase, true density, or grain density (ρ_s) was calculated for each sample by using [31]

$$\rho_s = \frac{\Sigma \rho_i V_i}{\Sigma V_i}, \tag{13}$$

where ρ_i and V_i are the true densities and volume fractions of constituent minerals.

It is also possible to establish a correlation [32,23] between bulk density or apparent and fractional porosity for the rock samples as

$$\rho_{\text{est}} = \rho_s\,(1 - \Phi) \tag{14}$$

where$\rho_s$was calculated from Eq. (13) and is found to be $2.914\,\text{g}\cdot\text{cm}^{-3}$ for all specimens. The estimated values of the bulk density are tabulated in Table I. As is evident from Table I, there exists excellent agreement between the experimental and estimated bulk densities. Table I also gives the measured values of the fractional porosity (Φ) which varies from 0.00322 to 0.00935.

Table II. Experimental Thermal Conductivity (λ), Thermal Diffusivity (κ), and Heat Capacity per unit Volume (ρC_P) of Gabbro Specimens along with the Standard Deviation (SD) at Normal Temperature and Pressure, using Air as Saturant

Specimen	λ ($W \cdot m^{-1} \cdot K^{-1}$)	SD	κ ($mm^2 \cdot s^{-1}$)	SD	ρC_P ($MJ \cdot m^{-3} \cdot K^{-1}$)	SD
Gb01	2.277	0.042	1.632	0.046	1.394	0.105
Gb02	2.302	0.061	1.531	0.061	1.504	0.097
Gb03	2.105	0.029	1.104	0.051	1.906	0.094
Gb04	2.093	0.048	1.377	0.049	1.521	0.087
Gb05	1.982	0.025	1.168	0.042	1.697	0.095
Gb06	2.092	0.053	1.238	0.056	1.688	0.124
Gb07	2.101	0.018	1.068	0.072	1.968	0.107
Gb08	1.876	0.049	1.015	0.049	1.846	0.130
Gb09	1.902	0.039	1.161	0.069	1.639	0.069
Gb10	2.053	0.028	1.129	0.054	1.820	0.107
Gb11	1.852	0.058	1.015	0.046	1.823	0.112
Gb12	1.845	0.060	1.148	0.078	1.606	0.104

Table III. Experimental Thermal Conductivity (λ), Thermal Diffusivity (κ) and Heat Capacity per unit volume (ρC_P) of Gabbro Specimens along with the Standard Deviation (SD) at Normal Temperature and Pressure, using Water as Saturant

Specimen	λ ($W \cdot m^{-1} \cdot K^{-1}$)	SD	κ ($mm^2 \cdot s^{-1}$)	SD	ρC_P ($MJ \cdot m^{-3} \cdot K^{-1}$)	SD
Gb01	2.497	0.051	1.612	0.050	1.561	0.102
Gb02	2.487	0.039	1.371	0.061	1.806	0.099
Gb03	2.471	0.042	1.331	0.048	1.845	0.078
Gb04	2.469	0.054	1.346	0.064	1.930	0.108
Gb05	2.448	0.048	1.431	0.047	1.823	0.098
Gb06	2.416	0.049	1.291	0.054	1.953	0.097
Gb07	2.470	0.026	1.196	0.061	1.651	0.108
Gb08	2.468	0.045	1.256	0.021	2.113	0.069
Gb09	2.416	0.060	1.221	0.037	1.937	0.067
Gb11	2.422	0.057	1.340	0.061	1.706	0.134
Gb12	2.435	0.037	1.098	0.054	2.189	0.105

4.2. Thermal Transport Properties

The thermal conductivity, thermal diffusivity, and heat capacity per unit volume of the samples along with the corresponding standard deviations are shown in Tables II and III using air and water as saturants, respectively. For air as the saturant in the pore spaces, the thermal

conductivity of the specimens ranges from 1.845 to 2.302 $W \cdot m^{-1} \cdot K^{-1}$, the thermal diffusivity ranges from 1.015 to 1.632 $mm^2 \cdot s^{-1}$, and the heat capacity per unit volume ranges from 1.394 to 1.968 $MJ \cdot m^{-3} \cdot K^{-1}$. For water as the saturant in the pore spaces, the thermal conductivity of the specimens ranges from 2.416 to 2.497 $W \cdot m^{-1} \cdot K^{-1}$, the thermal diffusivity ranges from 1.098 to 1.612 $mm^2 \cdot s^{-1}$, and the heat capacity per unit volume ranges from 1.561 to 2.189 $MJ \cdot m^{-3} \cdot K^{-1}$. It is obvious that the thermal conductivity increases for water-saturated samples. This is because the thermal conductivity of water is about 30 times larger than the thermal conductivity of air. Thus, our observations have the expected behavior. In the rest of the discussion, only the experimental data of the thermal conductivity and its prediction from different empirical models (both from existing and proposed) will be considered.

Under ambient conditions, the thermal conductivity values of calcium-rich plagioclase feldspars, pyroxene, olivine, and amphibole are 1.68, 4.41, 4.83, and 3.65 $W \cdot m^{-1} \cdot K^{-1}$, respectively [30]. Thus, by using Eq. (1), λ_s was calculated for each specimen of gabbro to be equal to 2.5 $W \cdot m^{-1} \cdot K^{-1}$.$\lambda_f$ is taken as 0.026 and 0.606 $W \cdot m^{-1} \cdot K^{-1}$ for air and water, respectively [33].

For gabbro specimens (using air as the saturant), in the Sugawara and Yoshizawa model, the empirical exponent n is taken as 1; for Asaad's model the empirical exponent c was calculated and its mean value is found to be 6.8; for the extended Veerendra and Chaudhary model, the empirical coefficient $\psi = 0.093$; for the Pande and Chaudhary model, $F = 3.8377$, and for our recent proposal, $m = 0.36$.

Similarly for water as the saturant, in the Sugawara and Yoshizawa model, the empirical exponent n is taken as 1; for Asaad's model the empirical exponent c is 1.93; for the extended Veerendra and Chaudhary model, the empirical coefficient $\psi = 0.017$; for the Pande and Chaudhary model, $F = 0.9554$, and for our recent proposal, $m = 0.67$.

From Table IV, it is noticed that with air as the saturant, Asaad's model gives an error up to 8%, and the Sugawara-Yoshizawa model gives a larger error compared to the other models and is about 33%. Veerendra-Chaudhary and Pande-Chaudhary models give errors up to 11%, whereas our recently proposed model, Eq. (10), gives an error of not more than 7%. For the case of water as the saturant, all the models give nearly similar results and the errors are within 2% (Table V).

Table IV. Experimental (λ_{exp}) and Effective (λ_e) Thermal Conductivities, Calculated by using Different Models, are given for Gabbro along with their Percentage Deviations (% Dev.) at Normal Temperature and Pressure, using Air as Saturant (Values of thermal conductivity are in $W \cdot m^{-1} \cdot K^{-1}$)

Specimen	λ_{exp}	Asaad's model (1955) [2]		Sugawara–Yoshizawa (1961) [6]		Veerendra–Chaudhary (1980) [12]		Pande–Chaudhary (1984) [14]		$\lambda_e = (1/\lambda_s + m\Phi/\lambda_f)^{-1}$ (2006) [25]		$\lambda_e = \lambda_s e^{-z\Phi \frac{\lambda_s}{\lambda_f}}$ (Proposed)	
		λ_e	% Dev.	λ_e	% Dev.	λ_e	% Dev.	λ_e	% Dev.	λ_e	%Dev.	λ_e	% Dev.
Gb01	2.277	2.262	0.7	2.484	09.1	2.058	09.6	2.047	10.1	2.249	1.2	2.264	0.6
Gb02	2.302	2.255	2.0	2.484	07.9	2.058	10.6	2.046	11.1	2.242	2.6	2.257	1.9
Gb03	2.105	2.199	4.5	2.480	17.8	2.054	02.4	2.045	02.9	2.187	3.9	2.202	4.6
Gb04	2.093	2.162	3.3	2.447	18.3	2.051	02.0	2.044	02.4	2.151	2.8	2.165	3.4
Gb05	1.982	2.051	3.5	2.469	24.6	2.043	03.1	2.040	03.0	2.048	3.3	2.055	3.7
Gb06	2.092	2.040	2.5	2.468	18.0	2.042	02.4	2.040	02.5	2.038	2.6	2.044	2.3
Gb07	2.101	1.960	6.7	2.462	17.2	2.036	03.1	2.038	03.0	1.967	6.4	1.965	6.5
Gb08	1.876	1.920	2.4	2.458	31.0	2.033	08.3	2.036	08.5	1.932	3.0	1.925	2.6
Gb09	1.902	1.917	0.8	2.458	29.2	2.032	06.8	2.036	07.1	1.929	1.4	1.922	1.0
Gb10	2.053	1.894	7.7	2.456	19.6	2.030	01.1	2.035	00.9	1.909	7.0	1.899	7.5
Gb11	1.852	1.888	1.9	2.456	32.6	2.030	09.6	2.035	09.9	1.904	2.8	1.892	2.2
Gb12	1.845	1.870	1.4	2.454	33.0	2.028	09.9	2.035	10.3	1.889	2.4	1.875	1.6

Table V. Experimental (λ_{exp}) and Effective (λ_e) Thermal Conductivities, Calculated by using Different Models, are given for Gabbro along with their Percentage Deviations (% Dev.) at Normal Temperature and Pressure, using Water as Saturant (Values of thermal conductivity are in $W \cdot m^{-1} \cdot K^{-1}$)

Specimen	λ_{exp}	Asaad's model (1955) [2]		Sugawara–Yoshizawa (1961) [6]		Veerendra–Chaudhary (1980) [12]		Pande–Chaudhary (1984) [14]		$\lambda_e = \left(1/\lambda_s + m\Phi/\lambda_f\right)^{-1}$ (2006) [25]		$\lambda_e = \lambda_s e^{-z\Phi \frac{\lambda_s}{\lambda_f}}$ (Proposed)
		λ_e	% Dev.	λ_e	% Dev.	λ_e	% Dev.	λ_e	% Dev.	λ_e	% Dev.	
Gb01	2.497	2.478	0.8	2.488	0.4	2.463	1.4	2.460	1.5	2.478	0.8	2.478 0.8
Gb02	2.487	2.477	0.4	2.487	0.0	2.462	1.0	2.460	1.1	2.477	0.4	2.478 0.4
Gb03	2.471	2.472	0.0	2.484	0.5	2.460	0.4	2.458	0.5	2.472	0.0	2.472 0.0
Gb04	2.469	2.468	0.0	2.482	0.5	2.458	0.4	2.456	0.5	2.468	0.0	2.468 0.0
Gb05	2.448	2.457	0.4	2.476	1.1	2.453	0.2	2.452	0.2	2.457	0.4	2.457 0.4
Gb06	2.416	2.456	1.6	2.475	2.5	2.452	1.5	2.452	1.5	2.456	1.6	2.456 1.6
Gb07	2.470	2.447	0.9	2.471	0.0	2.449	0.9	2.449	0.9	2.447	0.9	2.447 0.9
Gb08	2.468	2.443	1.0	2.468	0.0	2.446	0.9	2.447	0.8	2.443	1.0	2.443 1.0
Gb09	2.416	2.442	1.1	2.468	2.1	2.446	1.3	2.447	1.3	2.442	1.1	2.442 1.1
Gb10	2.423	2.440	0.7	2.466	1.8	2.445	0.9	2.446	1.0	2.440	0.7	2.440 0.7
Gb11	2.422	2.439	0.7	2.466	1.8	2.445	0.9	2.446	1.0	2.439	0.7	2.439 0.7
Gb12	2.435	2.437	0.1	2.465	1.2	2.444	0.4	2.445	0.4	2.437	0.1	2.437 0.1

4.2.1. Exponential Decay Expression for Thermal Conductivity Prediction

An exponential decay expression may also be used to predict the thermal conductivity of consolidated porous media at room temperature and normal pressure,

$$\lambda_e = \lambda_s e^{-z\Phi\frac{\lambda_s}{\lambda_f}} \tag{15}$$

where z is the empirical exponent whose value can be determined using any number of experimental values of thermal conductivity and corresponding values of Φ and λ_s, by

$$z\sum\left(\Phi\frac{\lambda_s}{\lambda_f}\right) = \sum \ln\left(\frac{\lambda_s}{\lambda_{exp}}\right) \tag{16}$$

For the case of gabbro specimens, the calculated value of z is 0.32 and 0.66 for air and water as saturants, respectively.

From Eq. (15), it is obvious that when Φ is equal to zero, λ_e becomes equal to λ_s, i.e., the thermal conductivity of the pure solid phase, as is the case of all other models, except for the Pande and Chaudhary model, where $\lambda_e \neq \lambda_s$ at $\Phi=0$.

The results obtained using this proposal are also given in Tables IV and V for air and water saturants, respectively; and the errors are up to 8 and 2% for air and water saturants, respectively.

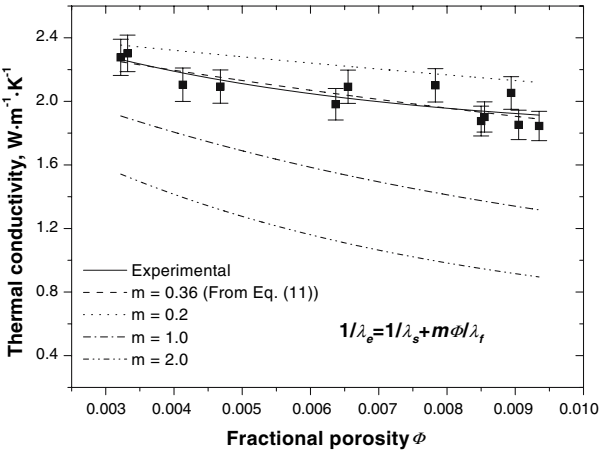

Fig. 1. Comparison of measured and predicted thermal conductivities of gabbro samples with air as saturant using different values of m.

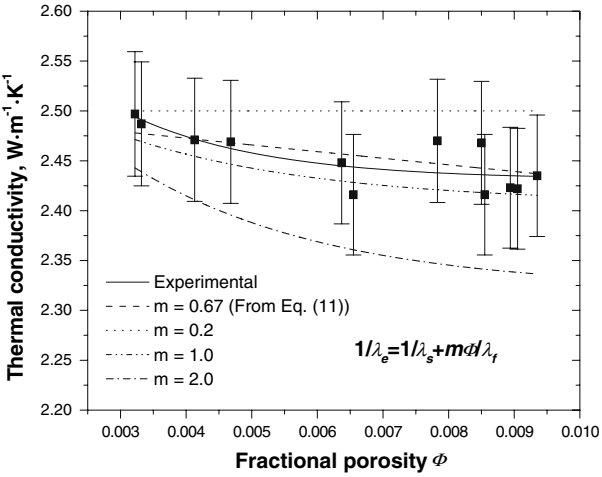

Fig. 2. Comparison of measured and predicted thermal conductivities of gabbro samples with water as saturant using different values of m.

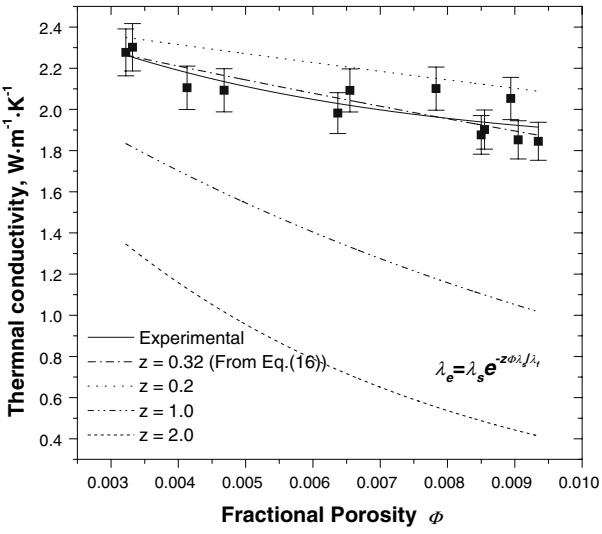

Fig. 3. Comparison of measured and predicted thermal conductivities of gabbro samples with air as saturant using different values of z.

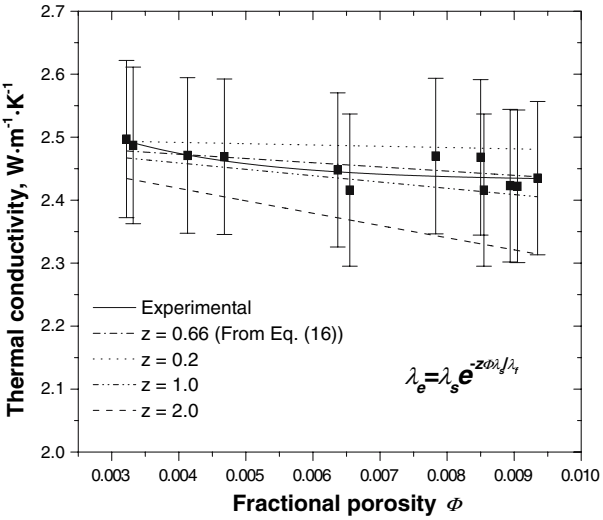

Fig. 4. Comparison of measured and predicted thermal conductivities of gabbro samples with water as saturant using different values of z.

The values of the thermal conductivity predicted using values of m and z other than those calculated from Eqs. (11) and (16) are also shown (Figs. 1–4). It is observed that the values of m and z calculated by using these equations gave the best results of all other randomly selected values which are 0.2, 1.0, and 2.0 in all cases.

5. CONCLUSIONS

The gabbro specimens have been characterized by mineral composition, porosity, and density. The ASTM standards have been applied to study the density-related properties. A simple correlation between density and porosity is established.

In this study, a step is taken to establish a previously proposed empirical model by using the experimental data of the thermal conductivity of gabbro specimens. The thermal conductivity of gabbro specimens has also been predicted by some existing empirical models. In addition, an exponential decay relation is tested which is equally good as the previously proposed model. It is noted that $\lambda_{exp}$and λ_e, predicted by the previously proposed empirical model are in agreement within 7% and the presently proposed exponential decay formula gives an error up to 8% for

air-saturated samples. For water as a fluid in the pore spaces, both models agree with the experimental data within 2%.

It is noted that in applying most of the empirical relations the adjustable parameters vary from material to material and from saturant to saturant. To check the applicability of these proposals, further work is in progress.

ACKNOWLEDGMENTS

The authors wish to thank Dr. M. Anis-ur-Rehman, Mr. Iftikhar Hussain Gul, Mr. Kashif Kamran, Mr. Zulqurnain Ali, Miss Samia Faiz Gurmani, Mr. Matloob Hussain (Earth Science Department, QAU) and Mr. Muhammad Saleem Mughal (Statistics Department, QAU) for their helpful discussion. The author (Aurangzeb) is grateful to the Higher Education Commission, Pakistan for supporting the doctoral studies.

REFERENCES

1. K. Lichtnecker, *Z. Phys.* **27**:115 (1926).
2. Y. Asaad, Ph. D. Dissertation, University of California, Berkeley, 1955.
3. A. A. Babanov, *Sov. Phys. Tech. Phys.* **2**:476 (1957).
4. W. D. Kingery, *J. Am. Ceram. Soc.* **42**:617 (1959).
5. A. Sugawara and Y. Yoshizawa, *Australian J. Phys*. **14**:468 (1961).
6. A. Sugawara and Y. Yoshizawa, *J. Appl. Phys*. **33**:3135 (1962).
7. A. D. Brailsford and K. G. Major, *Br. J. Appl. Phys.* **15**:313 (1964).
8. J. Huetz, *Progress in Heat and Mass Transfer* (Oxford, Pergamon, 1970).
9. E. Gomma, Ph. D. Dissertation, University of California, Berkeley, 1973.
10. A. E. Beck, *Geophysics* **41**:133 (1976).
11. H. Ozbek, Ph. D. Dissertation, Univ. of California, Berkeley, 1976.
12. K. Vareendra and D. R. Chaudhary, *Ind. J. Pure Appl. Phys.* **18**:984 (1980).
13. A. Ghaffari, Ph. D. Dissertation, University of California, Berkeley, 1980.
14. R. N. Pande and D. R. Chaudhary, *Pramana* **22**:63 (1984).
15. R. W. Zimmerman, *J. Pet. Sci. Eng.* **3**:219 (1989).
16. K. Misra, A. K. Shrotriya, R. Singh, and D. R. Chaudhary, *J. Phys. D: Appl. Phys*. **27**:732 (1994).
17. A. Bouguerra, J. P. Laurant, M. S. Goual, and M. Queneudec, *J. Phys. D: Appl. Phys.* **30**:2900 (1997).
18. K. J. Singh, R. Singh, and D. R. Chaudhary, *J. Phys. D: Appl. Phys.* **31**:1631 (1998).
19. A. Bouguerra, *J. Phys. D: Appl. Phys.* **32**:1407 (1999).
20. I. H. Gul and A. Maqsood, *Int. J. Thermophys.* **27**:614 (2006).
21. S. C. Hurlbut, *Dana's Manual of Mineralogy* (John Wiley & Sons, New York, 1971).
22. S. E. Gustafsson, *Rev. Sci. Instrum.* **62**:797 (1991).
23. W. H. Somerton, *Thermal Properties and Temperature Related Behaviour of Rock/Fluid Systems* (Elsevier, New York, 1992).
24. W. Woodside and J. H. Messmer, *J. Appl. Phys*. **32**:1688 (1961).

25. Aurangzeb, Z. Ali, S. F. Gurmani, and A. Maqsood, *J. Phys. D: Appl. Phys.* **39**:3876 (2006).
26. S. E. Gustafsson, E. Karawacki, and M. N. Khan, *J. Phys. D: Appl. Phys.* **12**:1411 (1979).
27. A. Maqsood, N. Amin, M. Maqsood, G. Shabbir, A. Mahmood, and S. E. Gustafsson, *Int. J. Energy Res.* **18**:777 (1994).
28. M. A. Rehman and A. Maqsood, *J. Phys. D: Appl. Phys.* **35**:2040 (2002).
29. M. Maqsood, M. Arshad, M. Zafarullah, and A. Maqsood, *Supercond. Sci. Technol.* **9**:321 (1996).
30. K. Horai and G. Simmons, *Earth Planet Sci. Lett.* **6**:359 (1969).
31. Y. S. Touloukian, W. R. Judd, and R. F. Roy, *Physical Properties of Rocks and Minerals* (McGraw-Hill, New York, 1981).
32. J. Anand, W. H. Somerton, and E. Gomaa, *Soc. Petrol. Eng*. J. **13**:267 (1973).
33. K. Horai, *J. Geophys. Res.* **76**:617 (1971).